ASSESSMENT OF WIDESPREAD FATIGUE DAMAGE IN THE PRESENCE OF CORROSION

UDC 539.388.1 620.193

G. Labeas, J. Diamantakos, Al. Kermanidis, Sp. Pantelakis

Laboratory of Technology and Strength of Materials
Department of Mechanical Engineering & Aeronautics
University of Patras, Patras 26500, Greece

Abstract. *Crack growth and residual strength prediction of aircraft structures under Widespread Fatigue Damage (WFD) condition is a very complex task, mainly due to the lack of appropriate analysis tools able to efficiently handle multiple interacting cracks. In the present work an integrated methodology based on the sub-structuring technique of the Finite Element Method and able to treat WFD problems is used. Theoretical predictions are in good agreement with experimental results. The complexity of the problem increases when the effect of corrosion has to be taken into account. Experimental results presented in this paper indicate that crack growth characteristics are not strongly affected by corrosion at the early and medium stages of propagation (Paris regime). Yet, with increasing crack length, crack growth rate increases rapidly for the corroded material. The implementation of the effect of corrosion in assessing fatigue life of corroded structures under Multiple Site Damage is discussed.*

1. INTRODUCTION

In April 1988 a Boeing 737 of Aloha Airlines with a service history of nearly 90.000 flights suffered an in-flight failure of a portion of the fuselage [1]. This structural failure was the result of a sudden linkup of small fatigue cracks emanating from adjacent rivet holes in the lap joint of the fuselage. The Aloha accident caused the Aircraft manufactures, the Airlines and the Federal Aviation Administration (FAA) to pay more attention to the issue of "Ageing aircraft", a technical term used to indicate that an aircraft is about to reach its original design goal. Consequently numerous committee meetings, International Conferences and research programs have been organized to study the structural integrity of the ageing airplanes [2-5]. The objective of these research and development programs is to produce basic knowledge and to develop technologies in order to ensure safety, extend the operation life and/or reduce the maintenance cost of an ageing aircraft structure.

Widespread Fatigue Damage (WFD) is a common phenomenon for ageing aircrafts. Multiple Site Damage (MSD) is one type of WFD and refers to the existence of interacting fatigue cracks at different sites of a structural component. It frequently occurs along the rows of fastener holes in aircraft wings and fuselage. MSD can become a very critical situation, as the sudden cohesion of interacting cracks may lead to catastrophic failure due to the further decrease of the residual strength of the structure [1, 6-7]. The simultaneous occurrence of corrosion and MSD at specific areas of the aluminium structure acts as an additional deteriorating parameter by affecting the residual strength and fatigue life. The computation of the fatigue life of an aging aircraft, with regard also to the corrosion-induced material deterioration is a task, which is currently very difficult to manage. Therefore despite the advancements in modeling fatigue crack growth and multiple site damage phenomena, the assessment of structural degradation in aging aircraft is still relying heavily on test data.

The prediction of crack-growth rate and residual strength of a cracked structure requires accurate calculation of the Stress Intensity Factor (SIF) at each crack tip. For problems concerning structures with simple geometry and few cracks (e.g. plates with one or two cracks) analytical solutions already exist [2]. As the number of cracks increases, or the geometry of the structure becomes more complicated, the formation of simple solutions becomes very difficult. The application of widely used Finite Element (FE) method is not a straight-forward procedure. Usually the part of the structure that should be analyzed to capture the interaction effects is complex and large while the cracks are of a quite smaller scale; it results to mesh difficulties and huge models. The iterative procedure, which is required for the calculation of the Stress Intensity Factors for different crack size combinations, leads to a further increase of the computation effort. To face the problem the sub-structuring procedure under the Finite Element (FE) method is utilized in the present paper. The proposed approach is based on the segmentation of the whole structure's model in FE super-elements. For each of these super-elements only the interface degrees of freedom (DOFs) are considered and a stiffness sub-matrix is calculated, related only to these DOFs. The solution of the problem then deals with the solution of the model containing the super-elements. A considerable reduction of the FE model size and CPU solution time is achieved, without affecting solution accuracy.

The occurrence of corrosion presents an additional significant cause of structural degradation in aging aircraft. Yet, the effect of existing corrosion on the structural integrity of aging aircraft still remains underestimated, although it has been recognized that the potential interaction of corrosion with other forms of damage such as wide spread cracking at regions of high stress gradients can result to loss of structural integrity and may lead to fatal consequences, [e.g. 1-2, 8]. Present day considerations of the corrosion induced structural degradation relate the presence of corrosion with a decrease of the load bearing capacity of the corroded structural member [8]. In [9] the effect of corrosion on multisite damage scenarios and aircraft structural integrity is considered such as to account for the onset of MSD from corrosion pits. In [10] corrosion-pitting damage has been quantified and related to the decrease in fatigue life of 2024-T351 specimens corroded in alternate immersion corrosion process. In [11] it was found that there is no significant effect of prior exfoliation corrosion on the fatigue crack growth rate of 2024-T351 specimens. Yet, recent investigations performed on a series of aircraft alloys have provided evidence that corrosion is not limited to the well known surface damage

process, which affects yield strength and fatigue life through the occurrence of corrosion notches, but is also the cause for a diffusion controlled material hydrogen embrittlement [e.g. 2, 4, 12-19]. This embrittlement is reflected into an appreciable reduction of energy density and fracture toughness of the embrittled area [15-16]. Hence, from the engineering viewpoint, corrosion and the associated corrosion induced hydrogen embrittlement are of essential interest as they affect the mechanical properties involved in fatigue analyses and residual strength calculations of aged aircraft structures. The prediction of residual strength and fatigue life of an aged and corroded aircraft structure requires the static, fatigue and crack propagation properties of the corroded material. They include the yield strength, which is necessary in the net-section yielding failure criterion, the S-N curves, the fatigue crack growth rate behavior and the fracture toughness, which is utilized in the prediction of unstable crack growth.

In the present work, an integrated methodology based on the sub-structuring technique of the Finite Element Method and able to treat WFD problems is used. Theoretical predictions are in good agreement with experimental results. Fatigue life and fatigue crack growth behaviour of corroded aluminium 2024 T351 alloy specimens have been experimentally investigated. For comparison, the tests have been also performed for the uncorroded material. The tests were carried out for as received bare, as well as, for anodised and sealed 2024 sheets.

2. SUPER-ELEMENT METHODOLOGY

An integrated methodology that we call "super-element" methodology was used for the treatment of MSD problems and is presented below. It includes stress analysis for the calculation of stresses and SIFs, computation of crack propagation, crack link-up, crack initiation and residual strength of the structure. Following the stress analysis technique as well as the post analysis calculations are briefly described. A more thorough presentation of the methodology may be found in [20].

2.1. Stress analysis using sub-structuring technique

For calculating fatigue crack growth rates by the common used rules (e.g. Paris law), accurate values of SIF range ΔK are needed. Also the computation of stresses at the regions of interest is necessary for crack initiation predictions. Moreover SIFs and stresses are essential for the application of crack link-up and residual strength criteria. Stress analysis and computation of SIFs of structures under WFD and MSD conditions is a very hard task to fulfil, mainly because of the complexity of the geometry under consideration. The problem becomes more difficult, when crack propagation has to be treated and therefore successive calculations are required. In Fig 1 a typical multi-cracked joint of aircraft fuselage is displayed. Generally, areas of interest include one or more rows and several columns of fastener holes.

In the present work a simple and accurate FE methodology, based on the sub-structuring technique [21-22] is proposed for performing stress analysis and SIF calculations. When applying the code, the shape of the area of the structure, which will be analysed, should be selected such that all possible crack interaction effects may be modelled.
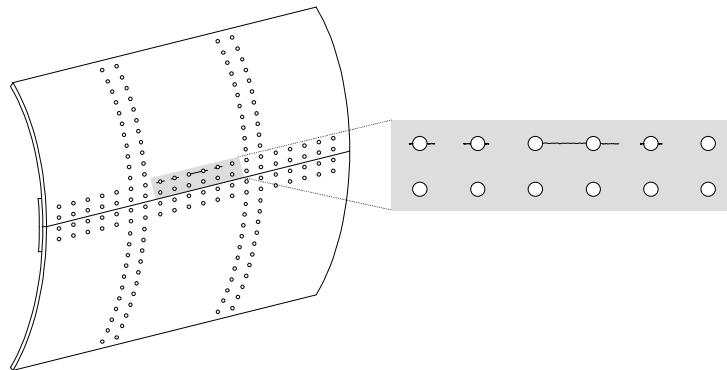
Fig 1. Typical aircraft structure with multiple cracks

For the application of the methodology the area of the panel, which contains cracks, is divided into suitable sub-structures and a corresponding super-element is developed for each one of them. The geometry of the sub-structures must be selected properly in order to meet two requirements. First, it should be possible for the full panel to be assembled mainly by repeated super-elements (like a "puzzle"). Second, changes in the geometry of the full panel, like crack propagation, should affect only one sub-area, so that the computational effort for calculating new super-elements is reduced. The repeatability of the whole panel's geometry is the feature actually making the super-element methodology practicable. The super-element geometric parameters depend on the geometry of the panel, e.g. the plate thickness, the horizontal and vertical pitch of the holes, the holes diameter, the distance from the side edge to the first hole and in cases where cracks exist, the corresponding crack lengths. For the modelling of common aircraft structures mentioned above nine basic forms of sub-structures are required, which are presented in Fig 2.
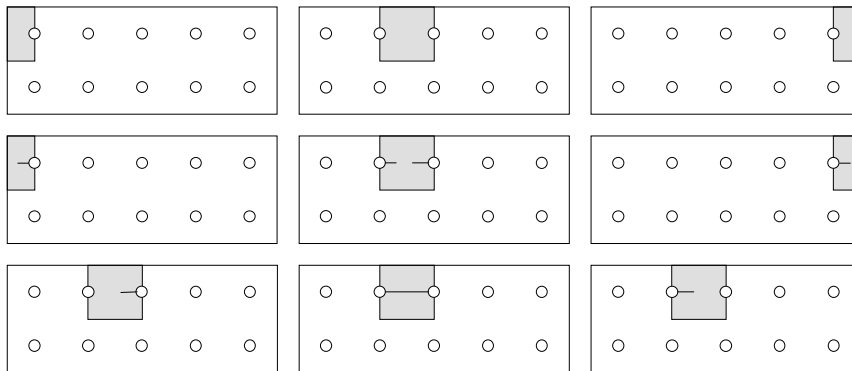
Fig 2. Basic forms of sub-structures

The complete panel is modelled using the appropriate super-elements. The part of the structure outside the holes' area is modelled by classic shell elements. Also two additional shell elements with very small stiffness are created at the side of each hole. These elements do not affect the stiffness of the panel but are essential because the FE code

used can compute stresses only by elements and not from distinguished nodes. The finite element model of the cracked MSD specimens, used in the present work, constituted by simple elements and super-elements as shown in Fig 3. Finally, the loads are applied on the model, it is solved and the stresses and SIFs are calculated at each point of interest.

(a)   (b)
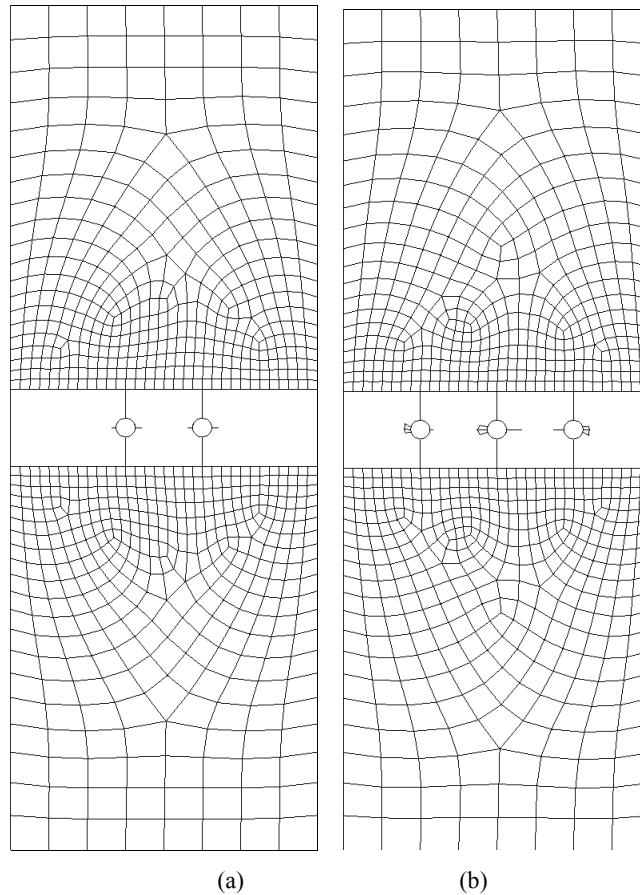
Fig 3. Typical model of the MSD specimens (a) Type I, (b) Type II

2.2. Accuracy and efficiency of the proposed methodology

In order to verify the computed results, a multiple cracked panel is analyzed using a full FE model and by the super-element methodology. It is an open-hole rectangular plate of dimensions 100×60x1mm with 3 rows and 5 columns of fastener holes. Each hole has a diameter of 4mm and two cracks of 5mm are emanating diametrically. The horizontal and vertical pitch is 20mm. The plate is clamped at its lower edge while a force of 20N is applied at the top of each hole, representing the rivet force. The two models are shown in Fig 4. It should be noted that the full model has 45585 nodes and 14850 elements, while the reduced model only 3060 nodes and 18 elements.
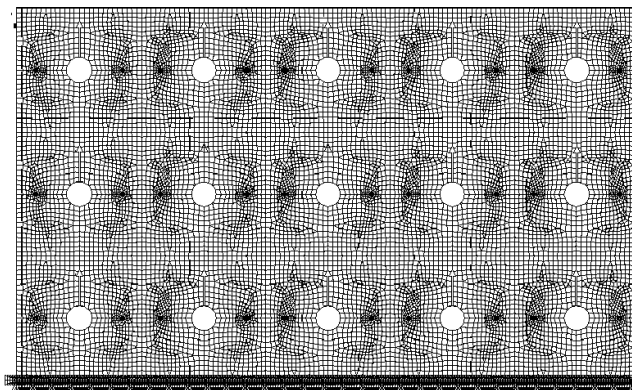
(a)
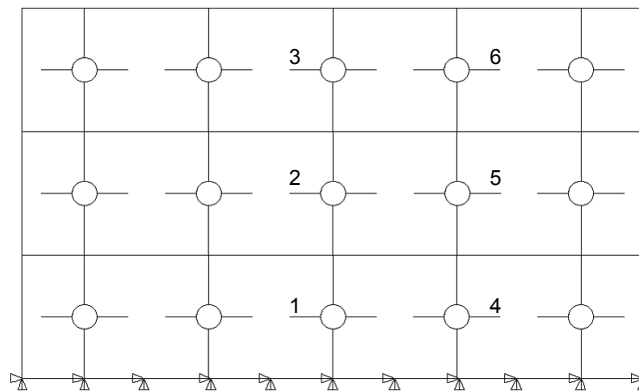
(b)

Fig 4. Model of the panel using classic finite elements (a) and super-elements (b)

The SIF results for the two models showed identical values. This coincidence of the numerical results can also be explained theoretically as it is proven that the super-element and the full model solutions are identical when, as least, all nodes of the interfaces between the super-elements are defined as Master DOFs. The benefits of the proposed methodology are clearly shown in Fig 5 where the CPU time is plotted as a function of the number of cracked holes modeled. The application of the substructuring technique results to a great reduction in CPU time. This reduction is particularly important in the cases of fatigue crack propagation, when the analysis for the determination of SIFs has to be repeated several times. The CPU time plotted for the reduced model includes the time required to generate the super-elements, to assemble the crack pattern and to solve the reduced model.
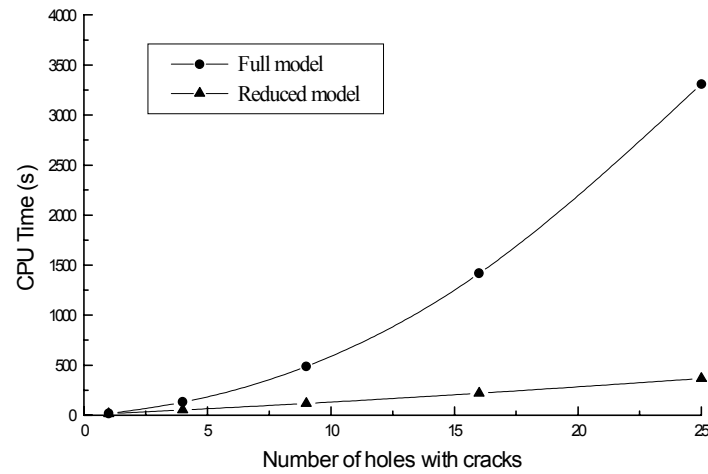
Fig 5. Efficiency of the method in terms of model size

2.3. Post-analysis calculations

After the solution of the finite element model and the computation of stresses at holes, some post-analysis calculations are performed. In order to retain the entire computational effort efficient, crack initiation and growth is treated incrementally. The approach concerning crack growth may be interpreted as the failure of material elements ahead of an existing crack after a certain critical number of fatigues cycles [23-24]. In practice, this consideration equals to the approximation of the continuously changing stress amplitude spectrum due to the stress redistribution through sufficient small loading intervals of constant stress amplitude. During each loading interval the crack pattern is considered as "frozen". Consequently stress distribution and SIFs are considered constant.

Crack growth

After the computation of SIFs, crack growth behavior of the structure can be computed by involving one of the well-established crack growth rules. In the present code, for simplicity, the well known Paris law:

$$\frac{da}{dN} = C \ (\Delta K)^n \tag{1}$$

is used, where C and n are materials constants. Obviously, any other fatigue crack growth rule may be also used.

Crack initiation

The occurrence of crack initiation depends on loading and material properties. However it exhibits a very stochastic nature [25]. In order to take into account the stochastic nature of crack initiation, in the proposed methodology a special technique has been derived. For each site of the structure a parameter is randomly assigned which is associated to the number of loading cycles, which are required for crack initiation at a

certain stress level. For each loading interval (i) the accumulated damage d_i is assumed to be the ratio of the number of loading cycles n_i of the interval (i), over the fatigue life N_i of the specimen at the corresponding stress level. Damage is accumulated according to Palmgren-Miner rule for the successive loading intervals, i.e.,

$$D = \sum_{i=1}^{i} d_i = \sum_{i=1}^{i} \frac{n_i}{N_i} \qquad (2)$$

Failure occurs when the damage parameter D equals unity. Then, it is assumed that at that certain site a crack of 1mm length is initiated.

Crack link-up

For the application of the present code, crack link-up is assumed to occur when the plastic zone of one crack reaches either the boundary of the next hole or the plastic zone of the next crack, known as the Swift criterion [26]. This assumption is commonly accepted [2, 27-28]. To apply the above link up criterion the plastic zone at each crack tip has to be estimated. The estimation can be made using optionally either the Dugdale's or the Irwin's formula, depending on the material.

Residual strength

After each crack pattern update the structure is checked for failure. The crack growth procedure is repeated for every initial crack scenario defined by the crack initiation module. Calculation of the residual strength of the structure requires special attention. Yet, as in the present work the aim is to develop the fatigue crack growth code, the oversimplified approach of the net-section yielding is used for completeness of the code. Finally, it should be noticed that as the developed fatigue crack growth model is deterministic, the probability of each computed crack growth pattern evolution to occur depends on the probability of each initial crack scenario to happen. In Fig 6 the flow chart of the super-element methodology is presented.
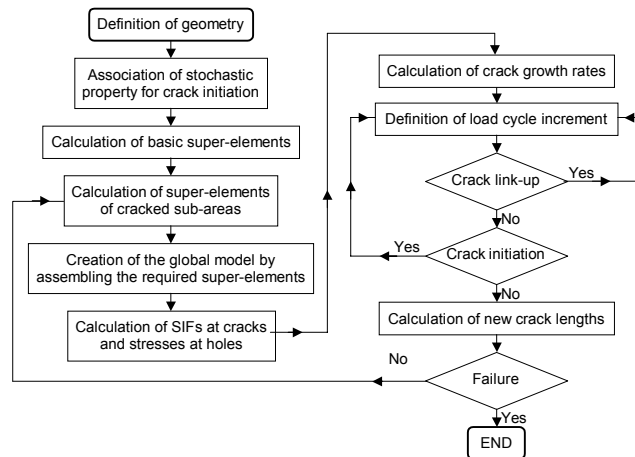
Fig 6. Flow-chart of the methodology

3. EXPERIMENTAL INVESTIGATION

The experimental investigation included fatigue, fatigue crack growth and MSD tests. S-N curves for anodised and sealed material were taken from [29] and are presented again here for completeness. Additional tests have been conducted in this work for bare material. Details about the tests specification can be found in [29]. Test coupons made of the aluminium alloy 2024 T351 were used for the fatigue crack growth tests. The alloy was received in sheet form with nominal thickness of 1.6mm. A portion of the 2024 T351 alloy was first coated with a hard anodisation layer and then sealed according to MIL-A-8625E before being corroded. Sealing was made by immersing the anodised specimens in a hot aqueous 5% sodium dichromate solution. Machining was made according to the specifications ASTM E 647-93. Prior to fatigue, some specimens have been subjected to exfoliation corrosion for 36 hours, according to the ASTM G 34-90 specification. This specific corrosive environment has been selected as it seems to satisfactory simulate the effect of long duration outdoor corrosion exposure on the material's mechanical properties [30]. The fatigue crack growth tests are summarized in Table 1 and were performed according to ASTM E 647-93. For the mechanical tests two servo hydraulic MTS machines of 100 and 250KN were used. All test were conducted at a frequency of 20Hz. During all fatigue crack growth tests, crack length was recorded via a DC Potential Drop measurement method.

Table 1. Fatigue crack growth tests performed on 2024 T351 Al alloy

Material treatment	Corrosion exposure prior to test	Maximum stress σ_{max} [MPa]	Stress Ratio $R=\sigma_{min}/\sigma_{max}$	Number of tests performed
As received	None	180.4	0.5	2
		176.1	0.7	2
	Exfoliation corrosion 36h	180.4	0.5	2
		176.1	0.7	2
Anodized and sealed	None	180.4	0.5	2
		176.1	0.7	2
	Exfoliation corrosion 36h	180.4	0.5	2
		176.1	0.7	2

The MSD specimens were made of 2024-T3 aluminium alloy QQ-A-250/4. The surface treatment was anodising and sealing per MIL-A-8625E, Type I, Class. Some of the specimens were pre-corroded. The geometric characteristics of the specimens are shown in Fig 7. The dimensions of all the specimens are 220mm height, 80mm width and 1.6mm thickness. These specimens were selected, as they are representative of the specimens used in MSD test programs [2]. In the centre area of each specimen open holes are manufactured with 5mm diameter and horizontal distance between holes centres 20mm. Two types of specimens were used: Type I with two open holes and two cracks emanating from each hole and Type II with three open holes and one crack emanating from each hole. Initial crack lengths (with reference to Fig 7) are presented in Table 2. All the MSD tests were performed on the 100 KN servo-hydraulic fatigue testing machine. All the specimens were fatigue loaded using a sinusoidal waveform at 5 Hz. The maximum stress was 100 MPa on the gross section, while the stress ratio was R = 0.1. An optical method was used for accumulating crack propagation data. It is based

on analysing images of the specimen by a computer. Images are grabbed during the fatigue crack propagation procedure by a suitable camera connected to the computer.
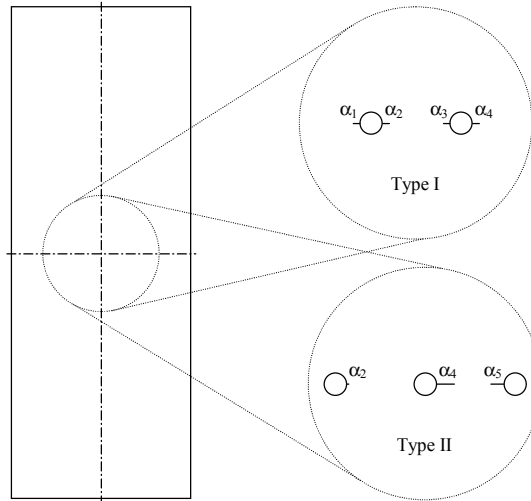
Fig 7. Geometric characteristics of MSD specimens

Table 2. MSD tests performed

Type of specimen	Crack lengths	Exposure to corrosive environment	No. of tests performed
I	$\alpha_1 \approx \alpha_2 \approx \alpha_3 \approx \alpha_4 \approx 1.5$ mm	No	6
		Yes	4
II	$\alpha_2 \approx 0.5$mm, $\alpha_4 \approx 4$mm, $\alpha_5 \approx 3$mm	No	3
		Yes	2

4. RESULTS AND DISCUSSION

4.1. Fatigue tests

Fig 8 shows the S-N curves derived for the material 2024 (bare and anodised and sealed) following exposure to exfoliation corrosion solution for 36 hours. In Fig 8(a) results for specimens with a hole ($K_t = 2.5$) are also presented. For comparison the S-N curves of the un-corroded alloys with and without anodising and sealing are included as well. The results show clearly that corrosion reduces fatigue resistance appreciably. Specimens including a hole ($K_t = 2.5$) show, as expected, reduced fatigue life as compared to specimens without a hole loaded at the same stress amplitude. As expected anodising process and sealing reduces the effect of corrosion. It is remarkable that the anodisation itself is reducing fatigue limit by almost 20%. This result is not intuitively understandable. The explanation for this behaviour may lay on the embrittlement due to hydrogen absorption occurring during the anodisation process. The classical interpretation of the above results relates the drop of fatigue life to the essential reduction of the fatigue crack initiation phase due to the

occurrence of corrosion notches. However, it is not clear yet if this is also the result of the ductility of the corroded material as has been reported in [29, 31].
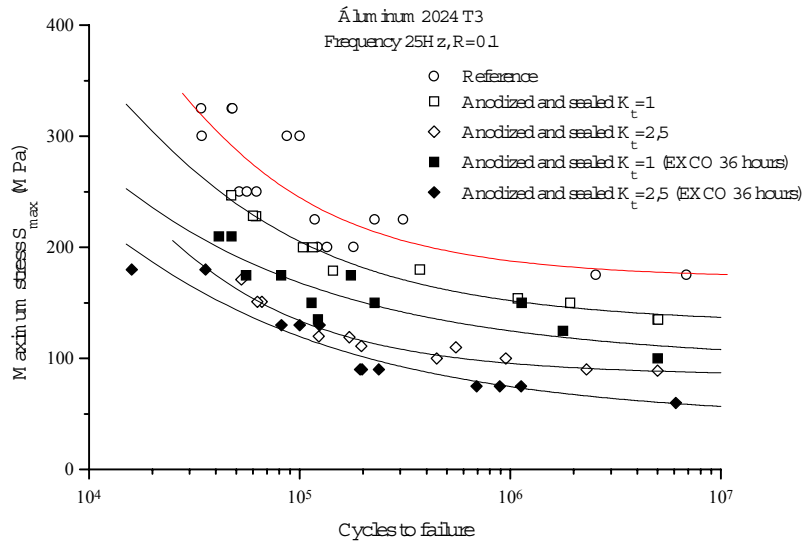
(a)
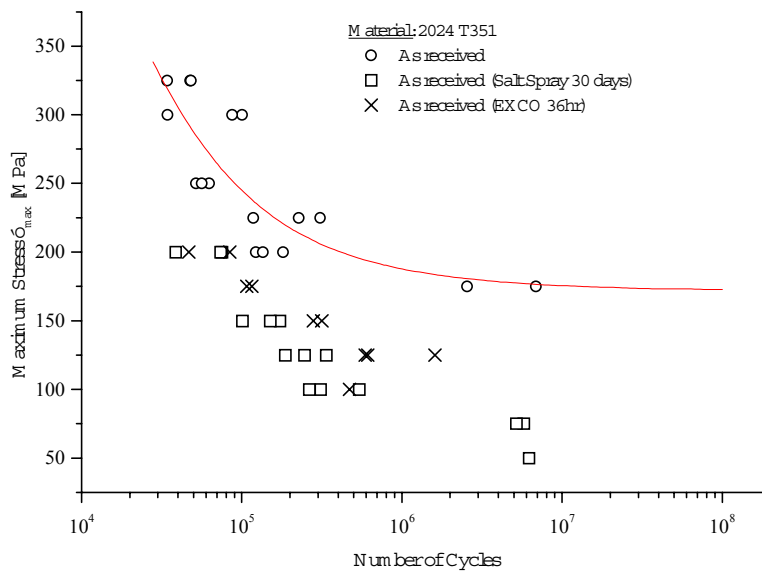
(b)

Fig 8. S-N curves for alloy 2024 T3 for (a) anodised and sealed and (b) bare material

The fatigue crack growth curves obtained for corroded and un-corroded specimens are displayed in Figs 9(a) and 9(b) for stress ratios 0.5 and 0.7, respectively. Each Fig

includes the fatigue crack growth curves derived for bare, pre-corroded bare, anodised and sealed as well as pre-corroded anodised and sealed specimens for the respective stress ratios. All curves in Fig 9 are the average of two tests.
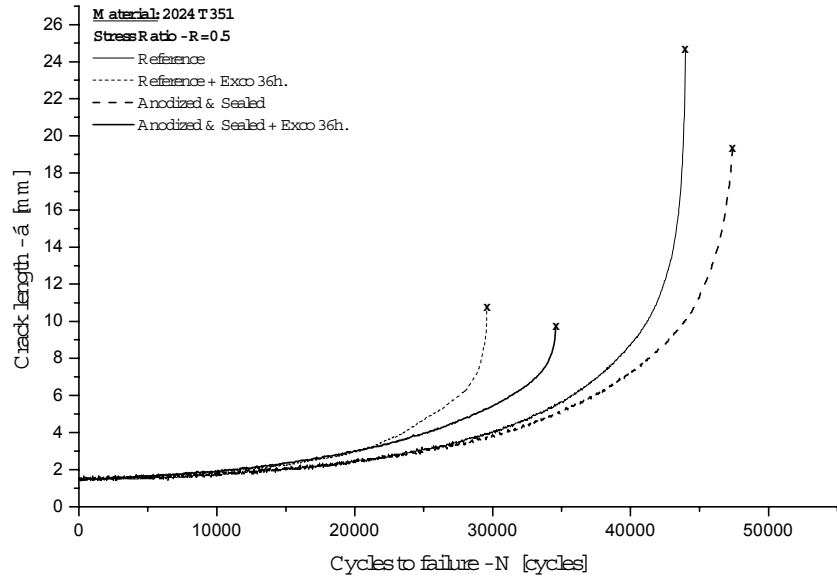
(a)
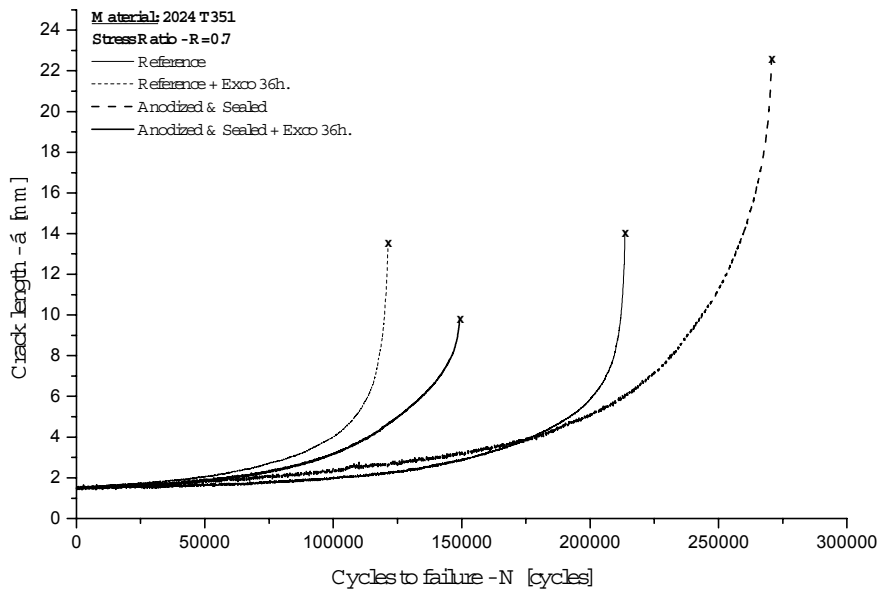
(b)

Fig 9. Fatigue crack growth tests for corroded and uncorroded 2024 T351 aluminium alloy specimens for R = 0.5 (a) and R = 0.7 (b)

The results indicate an appreciable reduction of the fatigue life for the corroded specimens. The fatigue life reduction for the investigated stress ratios can be seen in Table 3. Bare and anodised not-corroded specimens show almost same fatigue crack growth behaviour. A previous exposure of the specimens to exfoliation corrosion solution degrades fatigue crack growth resistance and life of the specimens. The corrosion induced material degradation is more severe for the unprotected bare specimens, as expected. It is noticeable that at the early stages of fatigue crack growth the effect of corrosion on the crack growth rate seems to be limited and increases with increasing crack length. The last point denoted in the experimental curves represents the crack length value measured just 1 sec before the failure of the specimen and it is denoted by a_{bf}. It is remarkable that this value is much lower for the corroded specimens. For the bare and pre-corroded specimens the reduction of a_{bf} has been 32.9% in average. This reduction is also appreciable (52.2%) for the anodised and pre-corroded material. The derived results should not be misinterpreted as a reduction in fracture toughness of the material. Running fractographic investigation will show whether the crack length of the corroded material at failure is indeed lower than the respective crack length of the uncorroded material, or if the corroded material behaves much more brittle in the last stage of fatigue crack growth.

Table 3. Fatigue crack growth test results

Stress ratio $R = \sigma_{min}/\sigma_{max}$	Maximum stress σ_{max} [MPa]	Material treatment	Corrosion exposure prior test	Cycles to failure N_f	a_{bf} [mm] (average)
0.5	180.4	As received	None	59100	22.20
			Exfoliation corrosion 36h	37000	9.57
		Anodised and sealed	None	66620	19.23
			Exfoliation corrosion 36h	53340	9.28
0.7	176.1	As received	None	275040	13.76
			Exfoliation corrosion 36h	168190	12.53
		Anodised and sealed	None	287260	20.70
			Exfoliation corrosion 36h	225780	9.81

4.2. MSD tests

The results of the MSD tests are shown in Figs 10(a) and 10(b) for type I and type II specimens, respectively. Results for both corroded and uncorroded specimens are presented as summarized in Table 2. Surprisingly, the comparison between fatigue crack growth for corroded and uncorroded specimens show no significant difference and the variation can be assumed to fall into the scatter observed in this kind of tests. It should be noted that fatigue crack growth in MSD situations depends not only on crack initiation and propagation but also on crack link-up. As the MSD specimens are pre-cracked, the initiation phase should not have any influence on the results. Furthermore, as shown before, there is no much difference between crack growth of corroded and uncorroded specimens in the early and medium stage of propagation (Paris regime). Due to the small distance between the adjacent holes, cracks are always propagating in this regime. One should, therefore, suggest that only

crack link-up will affect fatigue crack growth of corroded specimens as compared to crack growth of uncorroded specimens in MSD situations examined in the present work. However, it is not expected that this would change significantly the fatigue life. Further investigation is needed in order to assess fatigue crack growth in corroded MSD panels for different distances between the adjacent holes.

(a)

(b)
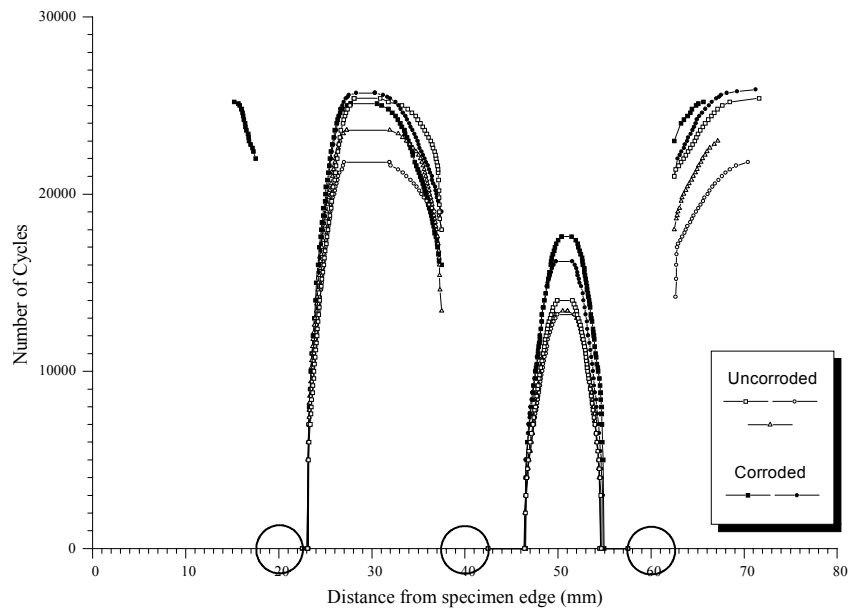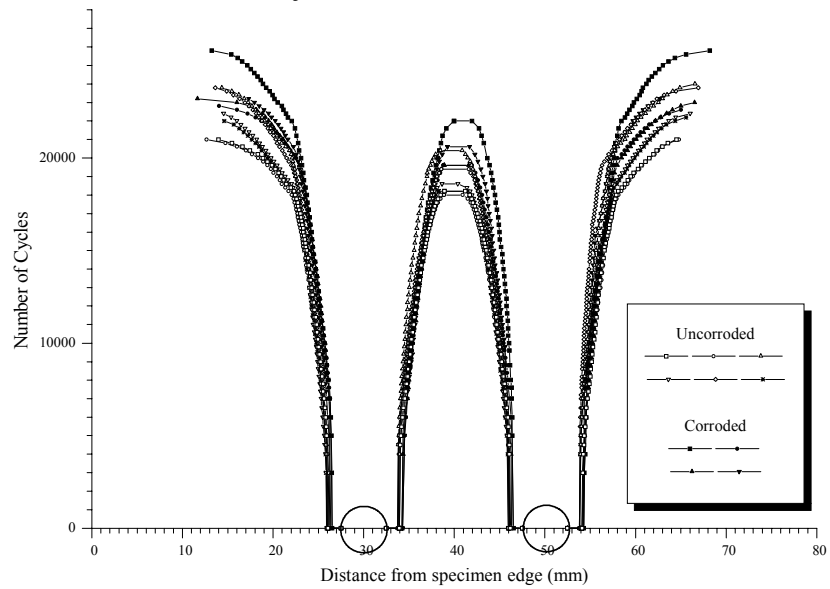
Fig 10. Fatigue crack growth test results for (a) type I and (b) type II MSD specimens

4.3. Crack growth prediction

Using the super-element methodology described before and the F.E. models shown in Fig 4, prediction of crack growth, initiation of new cracks and crack link-up can be made. The comparison between the theoretical predictions and the experimental results are shown in Figs 11(a) and 11(b) for one of the tested type I and type II specimens, respectively. The simulated MSD evolution follows the pattern of the experimentally obtained
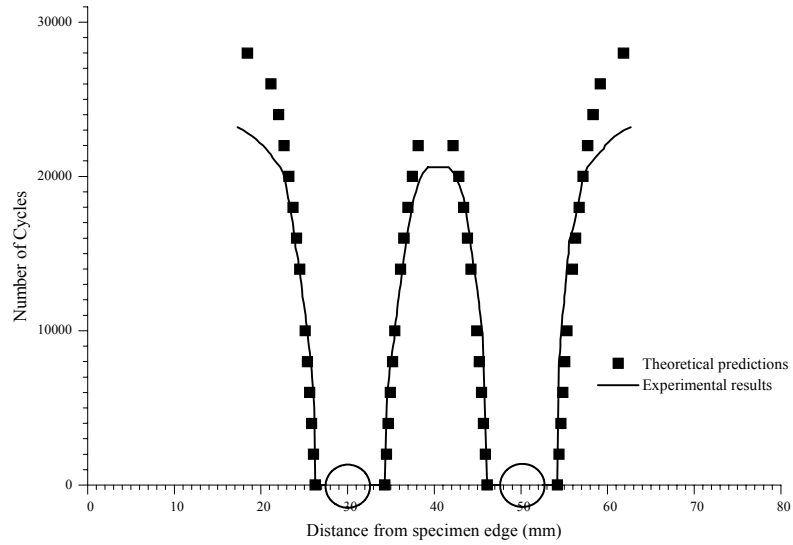
(a)
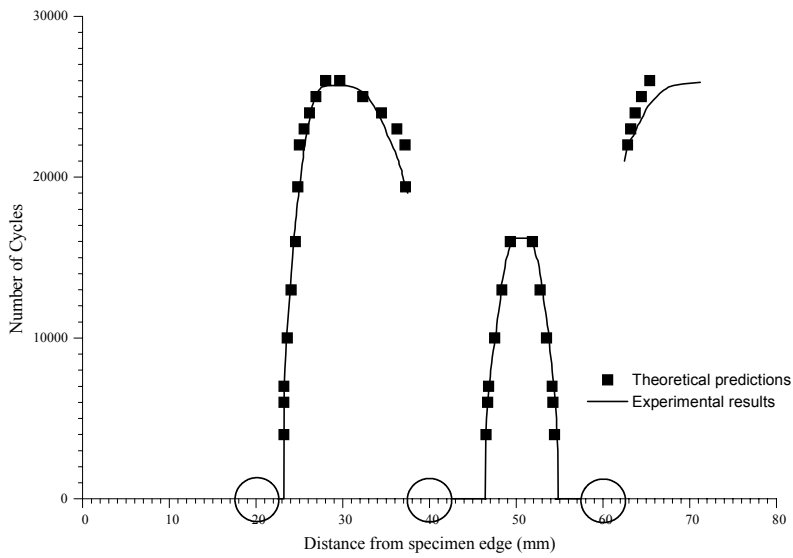
(b)

Fig 11. The comparison between the theoretical predictions
and the experimental results for (a) type I and (b) type II specimens.

MSD evolution sufficiently close. The small deviation observed is common even when a full FE model has been used [e.g. 28], as the simulation results are sensitive to Paris law constants used. The present simulation is advantageous in terms of computational effort and accuracy. It should be noted that the prediction in the presence of corrosion would lead to the same results, since Paris constants remain the same. Yet, referring to the discussions made above, this remark should not be interpreted as insignificance of corrosion for MSD issue.

5. CONCLUSIONS

A comprehensive experimental and theoretical investigation has been carried out to assess widespread fatigue damage in the presence of corrosion. The following conclusions can be made:

- − Corrosion reduces fatigue resistance appreciably
- − Crack growth characteristics are not strongly affected by corrosion at the early and medium stages of propagation (Paris regime)
- − The proposed Super-Element methodology can reliably and efficiently assess MSD evolution
- − Extensive investigation is still needed to recognise the exact effects of corrosion on MSD and to develop tools for quantifying this effect.

REFERENCES

1. Hendricks, W.R., (1991), The Aloha Airlines accident - a new era for aging aircracft, In Structural Integrity of Aging Airplanes, (Atluri, S.N., Sampath, S.G., Tong, P., editors), Springer-Verlag Berlin, Heidelberg, pp. 153-166.
2. BRITE-EURAM No BE 95-1053, Structural Maintenance of Ageing Aircraft, Final Report, Brussels, (1996).
3. Proc of the 20th Symposium of the International Committee on Aeronautical Fatigue, 14-16 July 1999, Bellevue, Washington, USA, (Rudd, J.L., Bader, R.M., editors), EPIC, Dayton, Ohio, USA.
4. Proc. of the FAA-NASA Symposium on the Continued Airworthiness of Aircraft Structures, Atlanta, Georgia, August 28-30 1996, (Bigelow, C., editor), National Technical Information Service, Springfield, Virginia 22161, USA, (1997).
5. Structural Integrity of Aging Airplanes, (Atluri, S.N., Sampath, S.G., Tong, P., editors), Springer-Verlag Berlin, Heidelberg, (1991).
6. Pártl, O., Schijve, L., (1992), Multiple-site-damage in 2024-T3 alloy sheet, Int. J. Fatigue, Vol. 15, No. 4, pp. 293-299.
7. Moukawsher, E.J., Grandt, A.F., Jr., Neussl, M.A., (1996), Fatigue life of panels with multiple site damage, J. Aircraft, Vol. 33, No. 5, pp. 1003-1013.
8. Inman, M.E., Kelly, R.G., Willard, S.A., Piascik, R.S., (1997), In Proc. of the FAA-NASA Symposium on the Continued Airworthiness of Aircraft Structures, Atlanta, Georgia, August 28-30, 1996, (Bigelow, C., editor), National Technical Information Service, Springfield, Virginia 22161, USA, pp. 129-145.
9. Bray, G.H., Bucci, R.J., Colvin E.L., and Kulak, M., (1997), Effect of prior corrosion on the S/N fatigue performance of Aluminum Sheet Alloys 2024-T3 and 2524-T3, In Effects of the environment on the initiation of crack growth, ASTM STP 1298, (Van Der Sluys, W.A., Piascik, R.S., and Zawierucha, R., editors), American Society for Testing and Materials, pp. 89-103.
10. Zamber, J.E., Hillberry, B., (1999), Probabilistic approach to predicting fatigue lives of corroded 2024-T3, AIAA Journal, vol. 37, pp. 1311-1317.

11. Chubb, J.P., Morad, T.A., Hockenhull, B.S., Bristow, J.W., The effect of exfoliation corrosion on the fatigue behaviour of structural aluminium alloys, In Structural Integrity of Aging Airplanes, (Atluri, S.N., Sampath, S.G., Tong, P., editors), Springer-Verlag Berlin, Heidelberg, pp. 87-97 (1991).

12. AGARD Workshop, Fatigue in the Presence of Corrosion, RTO Meeting Proceedings 18, Corfu, Greece, 1999.

13. EPETII/30 (1999). Damage Tolerance Behavior of Corroded Aluminum Structures. Final Report, General Secretariat for Research and Technology, Greece.

14. Smiyan, O.D., Coval, M.V., Melekhov, R.K. , (1983), Local corrosion damage of aliminum alloys, Soviet materials science, vol. 19, pp. 422-426.

15. Pantelakis, Sp., Vassilas, N., and Daglaras, P., (1993), Effects of corrosive environment on the mechanical behaviour of the advanced AL-LI alloys 2091 and 8090 and the conventional aerospace alloy 2024, Metall, vol. 47, pp. 135-141.

16. Scamans, G.M., Alani, R., Swann, P.R., (1976), Pre-exposure embrittlement and stress corrosion failure in Al-Zn-Mg alloys, Corros. Sci,vol. 16, pp. 443-459.

17. Tuck, C.D.S., (1980), Evidence for the formation of Magnesium Hydride on the grain boundaries of Al-Mg and Al-Zn-Mg Alloys during their exposure to water Vapour, In: Proceedings of the 3rd Int. Conference of Hydrogen on the Behavior of Materials, Jackson, Wyoming, USA, pp. 503-510.

18. BRITE/EURAM BE92-3250, Investigation on Aluminium-Lithium Alloys for Damage Tolerance Applications, Final Report, CEC Brussels, 1993.

19. Pantelakis, Sp.G., Kermanidis, Th.B., Daglaras, P.G. and Apostolopoulos, Ch.Alk. (1998). In: *Fatigue in the Presence of Corrosion*, AGARD Workshop, Corfu, Greece.

20. Diamantakos, I.D., Labeas, G.N., Pantelakis, Sp.G. and Kermanidis, Th.B., (2001), A model to assess the fatigue behaviour of ageing aircraft fuselage, Fatigue Fract Engng Mater Struct, vol 24, pp. 677-686.

21. ANSYS User's manual, Swanson Analysis Systems, Inc., (1989).

22. Gallaher, R.H., (1975), FE analysis fundamentals, Prentice Hall, Inc., New Jersey.

23. Pantelakis, Sp.G., Kermanidis, Th.B., Pavlou, P.G., (1995), Fatigue crack growth of retardation assessment of T2024-T3 and 6061-T6 aluminum specimens, Ther. Appl. Fract. Mech., vol. 22, pp. 35-42.

24. Sih, G.C., Chao, C.K., (1984), Fatigue initiation in un-notched specimens subjected to monotonic and cyclic loading, Theor. Appl. Fract. Mech., vol. 2, pp. 67-73.

25. Dowling, N., (1993), Mechanical behaviour of materials, Prentice Hall Int.

26. Swift, T., (1992), Damage tolerance capability, Specialists conference on fatigue of aircraft materials, Delft University of Technology.

27. Pitt, S., Jones, R., (1997), Fatigue damage in aging aircraft, Engng Failure Anal, vol. 4, pp. 237-257.

28. Silva, L.F.M., Goncalves, J.P.M., Oliveira, F.M.F., de Castro, P.M.S.T., (2000), Multiple site damage in riveted lap-joints: Experimental simulation and finite elements prediction, Int. J. Fatigue, vol. 22, pp. 319-338.

29. Pantelakis, Sp.G., Haidemenopoulos, G.N., (2002), Corrosion and hydrogen embrittlement of aircraft aluminum alloys, In Proceedings of International Conference on Mesomechanics, Aalborg University, Denmark, August 26-30, (Pyrz, R., Schjodt-Thomsen, J., Rauhe, J.C., Thomsen, T., Jensen, L.R., editors), pp. 619-626.

30. Jeong, D.Y., Orringen, O. and Sih, G.C. (1995), *J. Theor. Appl. Fract. Mech*., 22, pp. 127.

31. Pantelakis, Sp.G., Daglaras, P.G., Apostolopoulos, Ch.Alk., (2000), Tensile and energy density properties of 2024, 6013, 8090 and 2091 aircraft aluminum alloy after corrosion exposure, J. Theor. Appl. Fract. Mech., vol. 33, pp. 117-134.

ODREDJIVANJE ŠIROKO RASPROSTRANJENOG OŠTEĆENJA USLED ZAMORA U PRISUSTVU KOROZIJE

G. Labeas, J. Diamantakos, Al. Kermanidis, Sp. Pantelakis

Napredovanje prsline i predvidjanje zaostale snage strukture letilica pri stanju široko rasprostranjenog oštećenja usled zamora (WFD) veoma je složen zadatak, prevashodno usled odsustva odgovarajućih sredstava analize kojim bi se efikasno moglo pozabaviti višestruke prsline koje jedna na drugu deluju. U ovom radu korišćena je integrisana metodologija zasnovana na tehnici podstrukturiranja metode konačnog elementa, i koja može da tretira WFD probleme. Teorijska predvidjanja slažu se sa eksperimentalnim rezultatima. Kompleksnost problema se

povećava kada treba uzeti u obzir i uticaj korozije. Eksperimentalni rezultati koji su prikazani u ovom radu ukazuju da na karakteristike napredovanja prsline korozija nema snažan uticaj na ranim i srednjim stupnjevima širenja (pariski režim). Ipak, uz porast dužine prsline, stopa napredovanja prsline se rapidno povećava za korodirani materijal. Razmatra se ostvarenje uticaja korozije pri odredjivanju trajanja pri zamoru korodiranih struktura pri oštećenju na više položaja.